Supplementary Information

The rate of asparagine deamidation in a monoclonal antibody correlates with hydrogen exchange rate at adjacent downstream residues

Jonathan J. Phillips[†‡], Andrew Buchanan[‡], John Andrews[‡], Matthieu Chodorge[‡], Sudharsan Sridharan[‡], Laura Mitchell[‡], Nicole Burmeister[‡], Alistair D. Kippen[‡], Tristan J. Vaughan[‡], Daniel R. Higazi[‡], David Lowe[‡*]

[†] Department of Chemical Engineering and Biotechnology, University of Cambridge, Cambridge, CB2 3RA, UK. [‡] MedImmune Ltd., Aaron Klug Building, Granta Park, Cambridge, CB21 6GH, UK.
*Correspondence to lowed@medimmune.com

Structural modeling and molecular dynamics simulations of mAb1 and mAb1' antibody Fv regions

The structures of mAb1 and mAb1' antibody Fv regions were generated using homology modelling methods using tools in Discovery Studio (Accelrys). First, a structural model of mAb1 antibody Fv region was generated using the following template structures found in the Protein Data Bank - 1w72 for the VL domain, 2g75 for the VH domain and 2a9n to obtain the relative orientation of the VH and VL domains in Fv. The Ramachandran plot statistics for the generated model are: 96.3% of the residues (total 227 for the entire Fv) in the allowed region, 3.1% in the marginally allowed region and 0.5% in the disallowed region. A model for the mAb1' antibody Fv region was generated by using the *in silico* mutagenesis tools in Discovery Studio to mutate the glycine at position 55 to an alanine. The Ramachandran plot statistics for this model generated are similar to those of the mAb1 Fv region model.

Further preparation of the structural models molecular dynamics (MD) simulations and the simulations all were performed using tools available in Discovery Studio. Before performing MD simulations the CHARMm forcefield was applied to the Fv model structures generated as described above. Then the system was solvated using an orthorhombic box and boundary of 15 Å from the protein atoms. Sodium and chloride ions were added to the system to a concentration of 0.145 M. The system was then minimised using Adopted Basis Newton-Raphson method (ABNR) algorithm for 2000 cycles. The temperature of the system was then increased from 50 to 300 K over 5 ps. Equilibration was then performed over a period of 100 ps using constant pressure making sure the temperature and energies of the system were stable at the end of the

equilibration step. A 10 Å cutoff was used for non-bonded interactions and Particle Mesh Ewald approach for electrostatics. Leapfrog Verlet was used for dynamics integration. Following the equilibration stage, NPT production dynamics of 2 ns were performed at 300 K using a 2 fs time-step and applying the SHAKE algorithm for hydrogen-containing bonds. Conformations at every 2 ps interval from the production stage were captured for analyses. All trajectory analyses were performed using tools available in Discovery Studio.

Molecular dynamics simulations of mAb1 and mAb1': To further investigate the conformational dynamics in CDRH2 and provide rationalization of the apparent commonality of the deamidation and the hydrogen-exchange pathways, molecular dynamics simulations were run for structural models of the antibody variable (Fv) domains. We attempted to find intermediate structures of backbone and sidechain of mAb1 and mAb1' sites *en route* to the critical cyclisation step of succinimide formation in the deamidation pathway. We analyzed the backbone and sidechain conformational details of the structural intermediates where both the backbone amide of the residue at position 55 is not hydrogen bonded and the N54 Cγ atom is closest to the backbone nitrogen of residue at position 55 as these structures are likely to have the most potential for both exchange and cyclisation. With glycine at position 55, in these structural intermediates, the N54 Oδ1 atom is hydrogen bonded to the backbone nitrogen of N56, whereas with alanine at position 55, the N54 sidechain is not hydrogen bonded to any protein atom (S.I.Figure 4). We also noticed that the mAb1 and the mAb1' peptide bond backbone conformations are completely different in these intermediates. The backbone amide of A55 is solvent-exposed and that of G55 points toward the protein interior. In addition,

we found that during the course of the simulation, the mAb1' peptide existed in conformations where the A55 backbone amide points to the protein interior suggesting that certain conformational strains may have been relieved. We did not find such distinct populations for the G55 backbone conformations. The average percent solvent accessibility over the entire 2 ns simulation for N54 is slightly higher (78%) in the NG variant compared to that in NA variant (72%), which has been documented to correspond with higher rates of deamidation and hydrogen-exchange for the former[1]. Interestingly, we also found that the average percent solvent accessibility over the entire simulation is higher for the G55 amino acid (81%) than that for A55 (75%).

Considering the existence of structural intermediates, where the N54 sidechain is stabilized in mAb1 but not in the mAb1' variant, and changes in the backbone conformation observed for A55 but not for G55, we suggest that specific conformational intermediates, which favor cyclisation, form in mAb1 but not in the variant, mAb1'. Furthermore, given the correlation between deamidation and protection factor, these intermediates may be common to cyclisation and hydrogen-exchange exchange reactions in mAb1. However, the observable timescales that can be sampled by molecular dynamics mean that it is difficult to infer mechanism on a rare autocatalytic process (k_{obs} ~10^{-5} – 10^{-6} s^{-1})

Supplementary materials and methods

Generation of IgG variants, expression and purification. Site directed mutagenesis was performed using the QuikChange system (Stratagene) according to the manufacturer's instructions. Oligonucleotides were designed to mutate mAb1 residues as required. The VH domain was cloned into a vector containing the human heavy-chain constant domains and regulatory elements

to express whole IgG heavy chains in mammalian cells. Similarly, the variable light (VL) domain was cloned into a vector for the expression of the human light-chain (λ) constant domains and into regulatory elements to express whole IgG light chains in mammalian cells. To obtain IgG proteins, we transfected the heavy-chain and light-chain IgG-expressing vectors into CHO mammalian cells using standard methods. IgGs were expressed and secreted into the medium. Harvests were pooled and filtered prior to purification. Individual IgGs were purified using Protein A chromatography. Culture supernatants are loaded onto an appropriately sized column of Ceramic Protein A (BioSepra) and washed with 50 mM Tris-HCl (pH 8.0) and 250 mM NaCl. Bound IgG was eluted from the column using 0.1 M sodium citrate (pH 3) and neutralized by the addition of Tris-HCl (pH 9). The eluted material was buffer exchanged into phosphate-buffered saline (PBS) using Nap10 columns (Amersham). The concentration of IgG was determined spectrophotometrically at 280 nm using an extinction coefficient based on the amino acid sequence of IgG.

PD-1:PD-L1 inhibition HTRF assay

A biochemical assay using Homogeneous Time Resolved Fluorescence resonance energy transfer (HTRF) technology was established to measure the binding of PD-1 to PD-L1 using europium cryptate conjugated PD-L1 molecule as the donor and biotin conjugated PD-1 with streptavidin-XL665 as the acceptor. PD-1-Fc was conjugated with EZ-Link Sulfo-NHS-LC-Biotin according to manufacturer's directions (ThermoFisher) and PD-L1-Fc was conjugated with Europium trisbipyridine NHS Cryptate according to manufacturer's directions (Cisbio). The PD-L1-europium cryptate conjugate assay dilution factor was determined by comparing the fluorescence emission

intensity with the supplied calibrator[2]. Biotinylated PD-1 was diluted to a concentration of 1 nM in assay buffer (phosphate-buffered saline [PBS], 0.8 M potassium fluoride, 0.1% bovine serum albumin [BSA]) and streptavidin XL665 was diluted to a concentration of 4 nM in the same tube. The mixture was incubated for 15 minutes. After incubation, 5 µL was added into a 384 white, shallow well, nonbinding plate (Corning). Test IgG samples were serially diluted in a ratio of 1:5 in PBS containing 0.1% BSA (ranging from 1111 nM to 0.1 pM) and 10 µL was added into duplicate wells. The wells used to define total binding had 10 µL of PBS added and into the wells used to define nonspecific binding (NSB) had 10 µL of anti-PD-L1 antibody (MedImmune) at 1000 nM added. Finally, 5 µL of the europium cryptate conjugated PD-L1 diluted in assay buffer was added into all wells. The plate was sealed and incubated overnight at room temperature, before the fluorescence was measured on an EnVision plate reader (PerkinElmer) using an excitation 320 nm (75 nm bandwidth) filter with the emission filters 665 nm (7.5 nm bandwidth) and 590 nm (20 nm bandwidth). The raw data was initially analyzed using the equation 665 nm / 590 nm * 10,000 and was then expressed as % DELTA F using the equation (sample ratio - negative control ratio / negative control ratio * 100), where the NSB wells were used for the negative controls. The % specific binding is calculated from the % DELTA F values using the following equation % specific binding = (Sample - NSB / Total - NSB) * 100. The data was then analyzed using GraphPad Prism 5.01 (GraphPad) with the following 4 parameter equation; Y = Bottom + (Top - Bottom) / (1 + 10^ ((LogIC50 - X) * HillSlope)). Where X is the logarithm of the sample concentration and Y is the % specific binding.

Synthesis of P1 peptide

The peptide was prepared by automated peptide synthesis on a Biotage parallel synthesizer (SYRO II) by standard solid phase peptide synthesis (SPPS) on Wang acid resin (Novabiochem, 0.4 mmol/g loading) with 9-fluorenylmethyl-oxycarbonyl (Fmoc) for protection of N-α-amino groups. Side-chain protecting groups were tert-butoxycarbonyl (Lys) and trityl (His). N-α-Fmoc-L-amino acids (8.0 equiv.) were coupled using O-(1H-6-Chlorobenzotriazole-1-yl)-1,1,3,3-tetramethyluronium (HCTU, 7.5 equiv.) as coupling agent and N,N-Diisopropylethylamine (12.0 equiv.) as base in NMP for 20 min. N-α-Fmoc deprotection was performed using piperidine-DMF (1: 5) for 5 min, followed by piperidine-DMF (1:5) for 15 min. The peptide acid was released from the solid support by treatment with a cocktail consisting of TFA (95%), TIPS (2.5%) and water (2.5%) for 2 h. The TFA solution was concentrated by rotary evaporation, precipitated with diethylether and the peptide isolated by centrifugation at 3500 rpm. The crude peptide was purified using a Waters X-Bridge C18 stationary phase (19 mm x 250 mm, 5µm) eluting at 17mL/min with a linear solvent gradient of 0-30% MeCN (0.1% TFA, v/v) in water (0.1% TFA, v/v) over 30 min using a Varian SD-1 Prep Star binary pump system, monitoring by UV absorption at 210nm.

Characterization was carried out by LC/MS. Analytes were chromatographed by elution on a Polaris C8 stationary phase (4.6 mm x 100 mm, 3µm) using a linear binary gradient of 10-30% MeCN (0.1% TFA, v/v) in water (0.1% TFA, v/v) over 15 min at 1.5 mL/min at ambient temperature.

S.I. Table 1. Potential deamidation sites in mAb2 CDRs.

	CDR1	CDR2	CDR3
V_H	DYGMS	GI**N$_{52}$**W**N$_{53}$**GDSTGYADSVKG	RVAFDS
V_λ	RASQGIR**N$_{31}$**Y LG	AASSLQS	LQDY**N$_{93}$**YPRT

Variable domains of the heavy chain (V_H) and light chain (V_λ) each contain three CDRs. Deamidation sequence liabilities **highlighted** and numbered according to Kabat *et al.*[3] The canonical NG motif is in red.

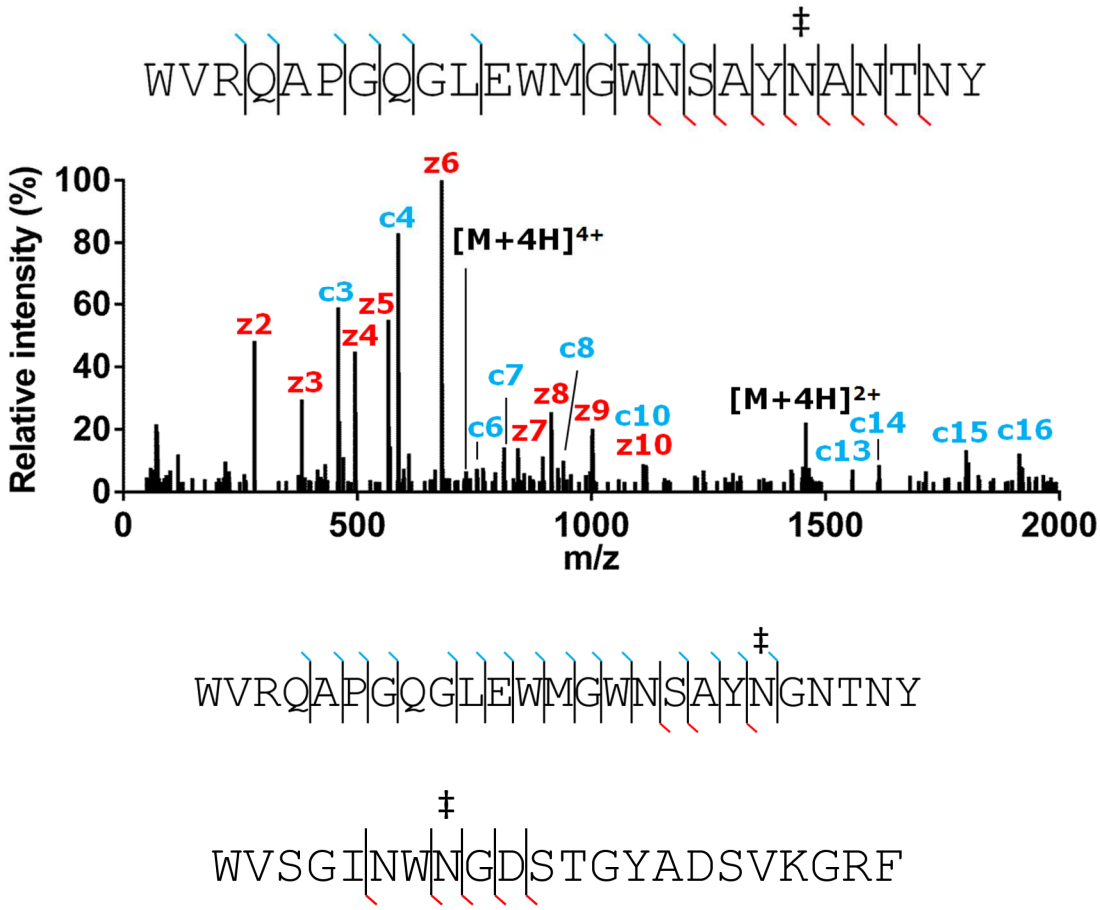

S.I. Figure 1

ETD fragmentation mass spectrum and sequence assignment for a CDRH2 peptide from mAb1' (upper panel). Peptide ion $[36\text{-}60]^{4+}$ was isolated in the quadrupole and the charge reduced species was observed at 1457.7 m/z, corresponding to the quadruply protonated, doubly charged ion. No other precursor ion was observed (position of 4+ species indicated for reference, but none was retained under conditions of ETD). Sequence ladders are shown for ETD of CDRH2 peptides from mAb1 ($[36\text{-}60]^{4+}$ ion – middle panel) and mAb2

([47-68]$^{3+}$ - lower panel). Blue tick - c-ion; red tick - z-ion; ‡ - site of deamidation (N54).

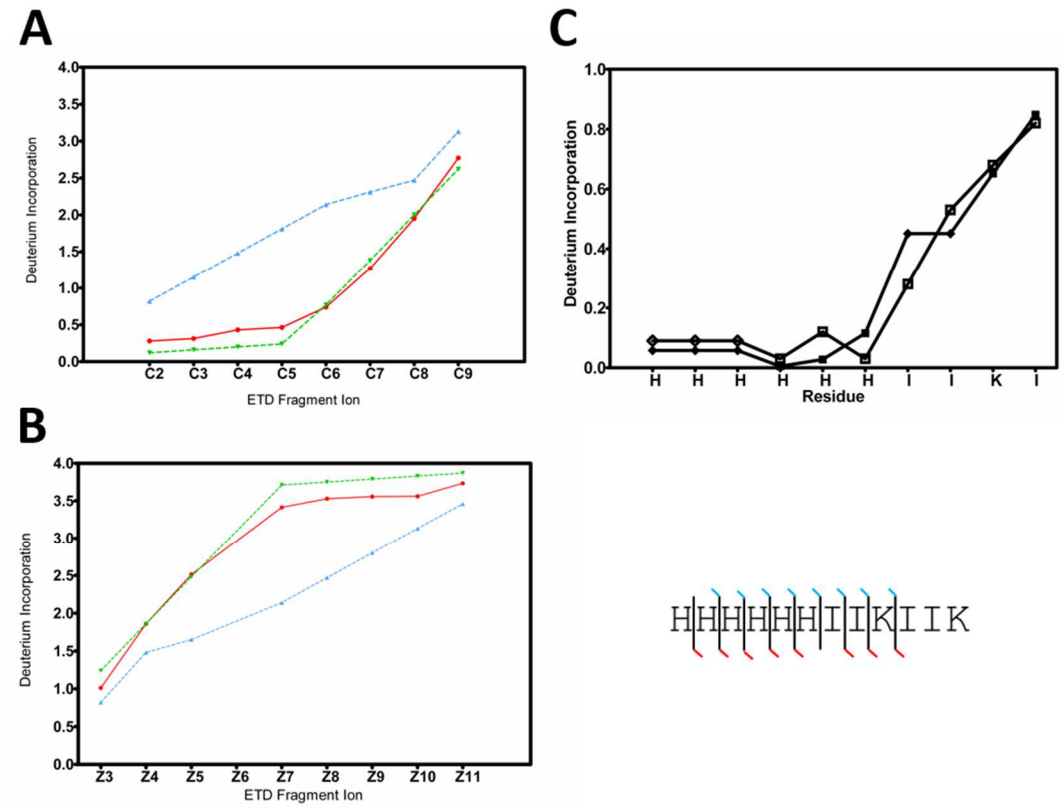

S.I. Figure 2

P1 peptide HDX-ETD-MS under identical quench, digestion, chromatography and mass spectrometry conditions as the antibodies. HDX-ETD-MS (red trace) of the c-ion series (a) and the z-ion series (b) both agree well with the calculated values for 0% scrambled deuterium incorporation (green trace) and not with the 100% scrambled values (blue trace). (c) As described by Rand and coworkers[4], deuterium is retained only in the residually structured C-terminal half of the peptide and not in the hexaHis N-terminal half, indicating that there is no scrambling of signal (P1 sequence: HHHHHHIIKIIK). Data were acquired by injection to a Waters HDX Manager system in line with

a G2 Synapt mass spectrometer under the same conditions as for analysis of antibody peptides. Site localized values were determined by subtraction of degenerate fragments. Where single-residue data was obscured by overlapping ion species that prevented full fragment ion coverage, an average value was taken. Sequence ladder is shown for ETD of P1 peptide. Blue tick - c-ion; red tick - z-ion.

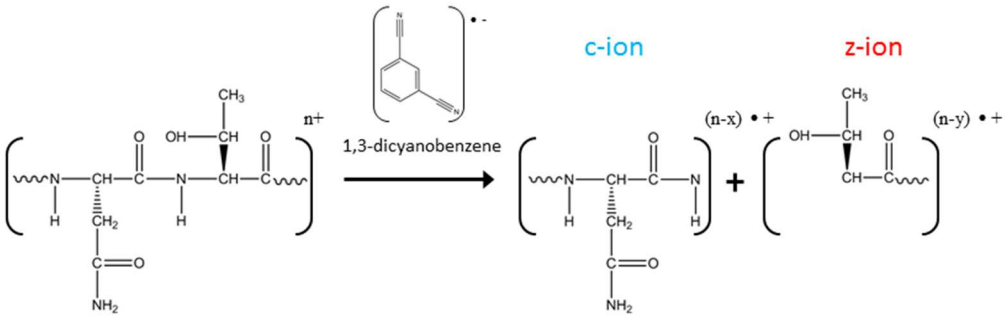

S.I. Figure 3

Fragmentation of the N-Cα bond of the polypeptide backbone to yield c-ions and z-ions, as typically observed in ETD experiments. The analyte precursor ion with n positive charges is reduced by the reagent radical anion, dicyanobenzene or 4-nitrotoluene, causing lysis preferentially at the N-Cα bond. The fragment c-ions and z-ions are observed with a fraction of the n charges, depending upon the relationship between charge reduction and the stability of the lysed bond. In the system studied, we observed principally 1+ and 2+ product ions resulting from 3+ or 4+ precursor.

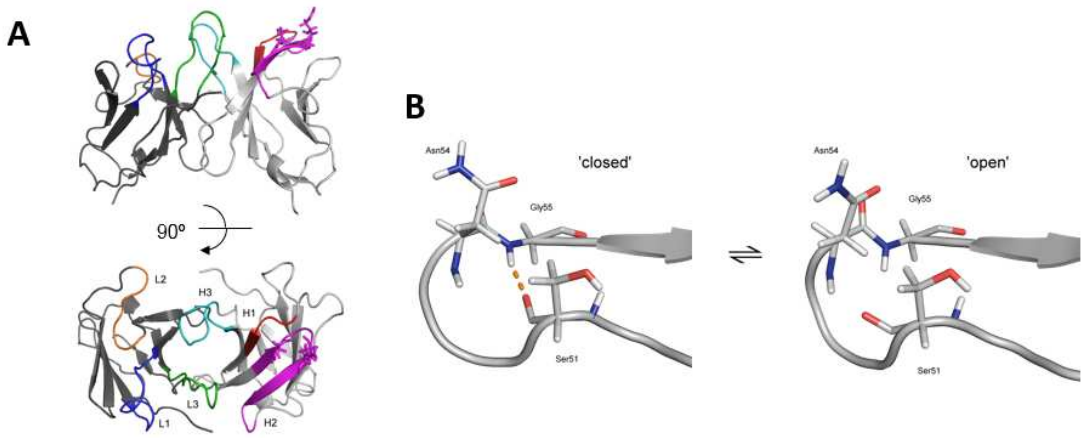

S.I. Figure 4

(A) Model of the variable domains of the mAb1 antibody ('NG' construct). The germline Asn54 and Gly55 and the Ser51 are shown as sticks. CDR loops are colored for reference and labeled H1-3, heavy chain; L1-3, light chain. In all simulated conformations of this model the sidechain of Asn54 is oriented into solvent.

(B) Detail of the CDRH2 region in sample conformations of a molecular dynamics simulation, illustrating possible 'open' [frame 199] and 'closed' [frame 310] states. H-bonds are indicated as dashed lines. The putative H-bond between the Gly55 nitrogen and the Ser51 carbonyl has a donor-acceptor distance of 2.7 Å in the 'closed' posture and is almost co-linear with an N-H-O angle of 162 degrees. The distance extends to 4.2 Å in the 'open' posture with an N-O-H angle of 142 degrees.

	N54
Y_0	-0.252 % ±3.52
Y_{max}	80.05 % ±5.109
k_{obs} (s^{-1})	2.60 x 10^{-6} ±0.0469
R^2	0.97

S.I. Table 1

Fitting values to equation 2 for the deamidation of N54 in mAb1. Y_0 and Y_{max} were unconstrained in fitting. Standard errors from the fitting are given. x is plotted in Fig. 1B with units of days. However, the observed kinetic rate constant is calculated in s^{-1} (i.e. scaled by 1/86400) to enable comparison with literature values.

	mAb1	mAb1'	mAb2
Y_0	0	0	0
Y_{max}	1.10 ±0.0327	1.06 ±0.0460	1.17 ±0.0545
k_{obs} (s^{-1})	1.48 x 10^{-2} ±0.0331	2.06 x 10^{-2} ±0.00418	4.51 x 10^{-2} ±0.0110
R^2	0.851	0.940	0.863

S.I. Table 2

Fitting values to equation 2 for the single amide H/D-exchange at the G/A55 nitrogen implicated in deamidation catalysis. Y_0 was constrained to zero and Y_{max} was unconstrained in fitting. Standard errors from the fitting are given.

mAb1

	k_{int}	k_{obs}	Pf
i-2	1.05E+02	7.09E-02 ± 0.02	3.17 ± 0.12
i-1	2.83E+01	4.12E-02 ± 0.01	2.84 ± 0.10
i	1.83E+02	7.06E-02 ± 0.02	3.41 ± 0.15
i+1	2.05E+02	1.99E-01 ± 0.15	3.01 ± 0.25
i+2	2.41E+02	5.72E-02 ± 0.02	3.62 ± 0.16
i+3	9.37E+01	3.89E-02 ± 0.02	3.38 ± 0.21
i+4	2.58E+02	5.57E-02 ± 0.02	3.67 ± 0.14
i+5	5.91E+01	5.21E-02 ± 0.02	3.05 ± 0.14

mAb2

	k_{int}	k_{obs}	Pf
i-2	9.59E+01	3.67E-02 ± 0.01	3.42 ± 0.06
i-1	4.28E+01	3.32E-02 ± 0.01	3.11 ± 0.10
i	1.26E+02	1.55E-02 ± 0.01	3.91 ± 0.20
i+1	2.05E+02	4.45E-02 ± 0.01	3.66 ± 0.07
i+2	3.91E+01	6.28E-02 ± 0.02	2.79 ± 0.14
i+3	8.16E+01	1.24E-03 ± 0.00	4.82 ± 0.54
i+4	8.95E+01	3.60E-02 ± 0.01	3.40 ± 0.12
i+5	1.56E+02	3.09E-02 ± 0.01	3.70 ± 0.15

mAb1'

	k_{int}	k_{obs}	Pf
i-2	1.05E+02	5.59E-02 ± 0.02	3.27 ± 0.15
i-1	2.83E+01	3.79E-02 ± 0.01	2.87 ± 0.10
i	1.83E+02	4.52E-02 ± 0.01	3.61 ± 0.14
i+1	1.10E+02	1.58E-02 ± 0.01	3.84 ± 0.16
i+2	1.63E+02	3.59E-01 ± 0.07	2.66 ± 0.09
i+3	9.37E+01	3.97E-01 ± 0.02	2.37 ± 0.03
i+4	2.58E+02	3.20E-01 ± 0.10	2.91 ± 0.13
i+5	5.91E+01	3.72E-01 ± 0.05	2.20 ± 0.07

S.I. Table 3

Calculated protection factors (Pfs) for CDRH2. k_{obs} values were determined by fitting single amide HDX-MS data to equation 2. k_{int} values were calculated in SPHERE from published standard data in unstructured peptides. Pf values were calculated from equation 4.

References

(1) Sinha, S.; Zhang, L.; Duan, S.; Williams, T. D.; Vlasak, J.; Ionescu, R.; Topp, E. M. *Protein Science* **2009**, *18* (8), 1573–1584.

(2) Mathis, G. *Clin. Chem.* **1995**, *41* (9), 1391–1397.

(3) Kabat, E. A.; Wu, T. T.; Perry, H. M.; Gottesman, K. S.; Foeller, C. *Sequences of Proteins of Immunological Interest. Public Health Service, US Department of Health and Human Services.*; 1991.

(4) Rand, K. D.; Pringle, S. D.; Morris, M.; Engen, J. R.; Brown, J. M. *J. Am. Soc. Mass Spectrom.* **2011**, *22* (10), 1784–1793.